Interfacial Conformations and Molecular Structure of PMMA in PMMA/Silica Nanocomposites. Effect of High-Energy Ball Milling

J. González-Benito*,† and G. González-Gaitano‡

Technological Institute of Chemistry and Materials "Alvaro Alonso Barba", Avda. Universidad 30, Leganés 28911 Madrid, Spain, and Departamento de Química y Edafología, Facultad de Ciencias, Universidad de Navarra, Pamplona 31080, Navarra, Spain

Received February 4, 2008; Revised Manuscript Received May 2, 2008

ABSTRACT: This work offers a new vision of the nanoparticle−polymer interface in inorganic nanoparticle filled thermoplastic nanocomposites in terms of macromolecular structure, conformations, and interactions. In particular, the molecular structure and interfacial conformation of PMMA in silica/PMMA nanocomposites obtained by high-energy ball milling (HEBM) have been studied. HEBM was applied to achieve an extraordinary dispersion of high content of silica nanoparticles within the PMMA polymer. Fourier transform infrared spectroscopy (FTIR) was used to investigate the effect that the important shear forces imposed by the HEBM process has on the PMMA structure and its dynamics and also the effect of the presence of silica nanoparticles inserted by HEBM on the particular conformations of PMMA appearing at the interface. It has been demonstrated that HEBM induces particular conformational changes on both the ester group and the backbone of the PMMA, which seem to be the cause of subsequent appearance of specific polymer chain packing at the interface.

1. Introduction

In recent years, organic polymer−inorganic particles nanocomposites have received great interest[1–9] since they can exhibit unique properties (thermomechanical, electrical, optical, etc.). However, generally, these improved or even unique properties can be only achieved if there is an adequate dispersion of the nanoparticles within the polymer matrix. Besides, it is generally accepted that to properly understand the influence of nanofillers in the final properties is necessary to get a perfect dispersion of nanoparticles with clear separation each other. In fact, the objective is usually to obtain the same interparticle distance with homogeneous interphases which, in the ideal case, would imply a perfect surface wetting by the polymer.

It is generally accepted that the so-called "interphase zone" plays an important role on inducing important changes on the properties observed in polymers filled with nanoparticles. The interphase zone is defined as the region surrounding each particle where the polymer chain dynamics may be altered due to intimate contact with the nanoparticles (resulting in restricted or enhanced mobility) plus the surrounding matrix influenced by that immediate layer.[10] In fact, the small size of nanoparticles makes the interfacial zone a so important fraction of the whole material that it can be considered as one of the proper constituents of the composite. However, specific analysis to adequately study the interphase region is not an easy task, and still considerable efforts should be focused on this issue.

Bansal et al.[11] have recently studied the thermal behavior of polymeric thin films to subsequently extrapolate their results to the thermal behavior of nanoparticles filled polymers. Their experiments are based on the hypothesis that the polymer close to the nanoparticles surface should behave in a similar way to that of a thin film of the same polymer deposited over a substrate with the same nature than that of the nanoparticles. However, several works have shown that the dynamics of a polymer surface may be quite different than that of the bulk,[12–16] and therefore new experiments should be carried out to reinforce the conclusions extracted from the experiments on thin films. Some researchers have tried to overcome this by studying model polymer nacomposites consisting of polymer films confined between silica plates,[9] for instance.

In general, two experimental results are found for the glass transition temperature, T_g, of polymer thin films: (i) T_g is a function of the thickness,[9,13,14,17–19] and (ii) T_g can change if polymer film is deposited on a substrate.[13,19] When the thickness of the polymer film decreases and favorable interactions between the polymer and the substrate exist, an enhancement or no change in the T_g has been usually found while, when the thickness decreases in a film with poor interaction polymer−substrate, a T_g decrease is observed. In the case of favorable interactions between the polymer and the substrate, experiments carried out with neutron reflectivity have shown that there exists an increase in the density gradient to the surface.[20,21] All these results seem to be related with the specific conformation adopted by the polymeric chains exactly at the surface of the substrate that allows better macromolecular packing. For example, there are studies pointing out the existence of conformational changes in the PMMA backbone on an aluminum surface[22] due to the existence of ionic bonds generated by the hydrolysis of ester groups over the aluminum surface. However, Grohens et al.,[23] based on the previous works of O'Reilly,[24] estimated the conformational energies at the interfaces using reflected infrared absorption spectroscopy discussing their results in terms of conformational changes due to the restrictions imposed by the surface to the chain motion.

At this point it seems opportune to take a further step by performing these studies in polymers filled with nanoparticles with the objective of investigating the influence of these fillers in the macromolecular conformations and, if possible, to understand their relation with the final properties of the "real" nanocomposite material. A paramount requirement must be fulfilled, i.e., the "perfect" dispersion of the nanoparticles within the polymer.

Recently, González-Benito et al.[25] have used high-energy ball milling (HEBM) as a method to mix a polymer with inorganic nanoparticles in the solid state, achieving an extraordinary dispersion of nanoparticles within the polymer. However, it is not clear yet what is the effect that the important shear forces imposed to the mixture provoke in the polymeric structure and,

* Corresponding author. E-mail: javid@ing.uc3m.es.
† Technological Institute of Chemistry and Materials "Alvaro Alonso Barba".
‡ Universidad de Navarra.

10.1021/ma800260k CCC: $40.75 © 2008 American Chemical Society
Published on Web 06/11/2008

finally, what kind of adhesion is achieved between the nanoparticles and the polymer. This has led us to consider two main objectives, by using FTIR spectroscopy, to determine what is the effect of the HEBM: (i) on the molecular structure of the polymeric chains of a commercial PMMA and (ii) on the macromolecular conformations at the silica nanoparticles/PMMA interface. This study should provide important information to understand which kind of interactions and arrangement between the macromolecules and nanoparticles are required to achieve such a good nanoparticle dispersion within the polymer as that one obtained by HEBM.[25]

In particular, it is well-known that an important molecular feature, which has been identified as contributing to certain physical properties, is the conformational energy (ΔH). Probably because of its simplicity, infrared spectroscopy has been the most widely used method to measure energy differences between conformational isomers and has been applied to polymers. Because of this, the simple use of IR spectroscopy was chosen for this work.

2. Experimental Section

2.1. Materials. Fumed silica nanoparticles (99.8% pure silica, 200 m^2/g surface area, 2.2 g/cm^3 density, and 14 nm diameter) were supplied by Sigma-Aldrich and atactic poly(methyl metacrylate), PMMA (Oroglas V852T), with density 1.19 g/cm^3, average number molecular weight $M_w = 75\,300$, and polydispersity index PDI = 1.5, was purchased from Atoglas S.A. Methyl ethyl ketone and tetrahydrofuran HPLC grade (Aldrich) were used as solvent of PMMA in the light scattering and size exclusion chromatography experiments, respectively.

2.2. Sample Preparation. PMMA pellets were first grinded in a MF 10 basic Microfine grinder drive (IKA WERKE) to obtain relatively fine PMMA particles. These were mixed with the fumed silica nanoparticles in a weight proportion of 10% of silica. Subsequently, about 20 g of mixture was introduced in a vial of alumina with 190 g of 20 mm diameter alumina balls. The vial was then hermetically closed and placed in a Pulverisette 5 Fritsch apparatus where the powder was milled (400 rpm) for 10 h at room temperature (high-energy ball milling, HEBM). To study the effect of the milling time along the blending process, samples of silica−PMMA were extracted at different milling times (1, 2, 4, 6, 8, and 10 h), leaving the equipment to rest 25 min every hour of active milling. On the other hand, to avoid excessive heating of the equipment as well as of the milled powders, a subcycle of milling was considered: every 6 min of active milling was followed by 3 min of resting. For later comparisons PMMA alone (without nanoparticles) was subjected to the same ball milling cycles.

The powders coming from the milling process were diluted in KBr (less than 1 wt %) to subsequently prepare tablets for being studied by FTIR spectroscopy. All the samples prepared had sufficiently low amount of PMMA or silica−PMMA to satisfy the Lambert−Beer law.

2.3. Experimental Techniques. The hydrodynamic radii of PMMA chains were obtained by dynamic light scattering (DLS) with a photon correlation spectrometer DynaPro MS/X by analyzing the autocorrelation functions by the cumulants method using the Dynamics V6 software. Samples were dissolved in methyl ethyl ketone (7 mg/mL) and filtered with syringe filters of 0.02 μm (Anotop) before the measurement. All experiments were carried out at 25 °C.

Size exclusion chromatography as a function of milling time (0, 4, and 10 h) was performed with a Shimadzu CTO-6A unit using a 515 HPLC pump of Waters and PLGel columns from Polymer Laboratories. Refractive index detection was performed at room temperature from 10 mg mL^{-1} polymer solutions in THF (20 μL injections at a flow rate of 1 mL min^{-1}) with a Shimadzu RID-6A refractometer.

FTIR spectra were recorded with a FT-IR Spectrum GX (Perkin-Elmer). Five scans and a resolution of 4 cm^{-1} were used. Spectra for each sample from 400 to 4000 cm^{-1} were taken at different temperatures within the interval 30−150 °C every 10 °C. The samples were heated in a SPECAC heater specifically designed for the FTIR equipment controlling the temperature with an accuracy of ±1 °C. The temperature stability was achieved after 5 min of hold on time.

Table 1. Absorption Peaks in *s*-PMMA (1050−1300 cm^{-1})

peak	frequency (cm^{-1})	Nagai's assignment[26]
ν_1	1268	ν_a(C−C−O) coupled with ν(C−O)
ν_2	1238	
ν_3	1192	skeletal stretching coupled with internal C−H deformation
ν_4	1148	
ν_5	1060	planar zigzag arrangement of the backbone carbon atoms

2.4. Characteristics of the PMMA Infrared Spectrum. Although still with very slight differences in the final interpretation, there have been many authors who did their particular assignations to the IR absorption bands of the infrared spectrum of PMMA. In particular, it is generally accepted that in the range between 1050 and 1300 cm^{-1} there are at least four absorption peaks associated with the ester group for syndiotactic poly(methyl methacrylate), *s*-PMMA,[26,27] which do arise from specific interactions.[27] The different possible rotational positions (PMMA conformations) of the ester group seem to yield different force constants (hence different peaks), so variations on the absorbances of those peaks should be related with the population of the different PMMA conformations. In Table 1 Nagai's assignation of the *s*-PMMA IR absorption bands observed in the interval 1050− 1300 cm^{-1} is collected.[26]

In the event for which two absorption peaks are due to the same vibration but the frequencies are different (the ester group can be found in either one of two different rotational positions, causing the force constants to be slightly different), the sum of the integrated absorbances for both peaks should not depend on the temperature, provided the absorbance per ester group is the same for both locations. On the other hand, the ratio of the absorbances for the two peaks should vary with temperature as the number of ester groups increases in one of the conformations (conformation i) at the expense of the number of ester groups in the other conformation (conformation $i + 1$). Therefore, a plot of $\ln [A(\nu_i)/A(\nu_{i+1})]$ vs $1/T$ (van't Hoff plot) should be a straight line if the population distribution between the two conformers is controlled by the Maxwell−Boltzmann statistics. Here $A(\nu_i)$ and $A(\nu_{i+1})$ represent the absorbances of the two peaks assigned to the same vibration in two conformations i and $i + 1$, respectively, and T is the absolute temperature. In fact, the absorption peaks at ∼1270 and ∼1240 cm^{-1} have been used habitually in the literature to calculate the van't Hoff conformational energies from the slopes of the van't Hoff plots.[28,29]

Other important bands for structural studies are those at 860 cm^{-1} characteristic for the all-trans or close to the all-trans (TT) conformation, while the trans−gauche one (TG) absorbs at 843 cm^{-1} and is characteristic of the random coil.[28,30]

3. Results and Discussion

3.1. Effect of HEBM on PMMA. DLS permits to obtain, from the intensity autocorrelation function, the size spectrum of the particles present in the sample. The analysis of this function can be carried out assuming a single relaxational mode by the cumulant method, yielding the mean size, expressed as the hydrodynamic radius, R_h, and the width of the distribution. The apparent radii and polydispersity, Γ, as a function of milling time for PMMA are plotted in Figure 1. Before the milling the mean radius is 7.8 nm, which reduces to 5.3 nm after 10 h of treatment. At the same time, the scattered intensity diminishes following the same trend, passing from 46 to 21 kcounts/s, as correspond to the smaller size of the polymer (data not shown). Although DLS experiments do not allow obtaining an absolute molecular weight, it is possible to estimate the relative change

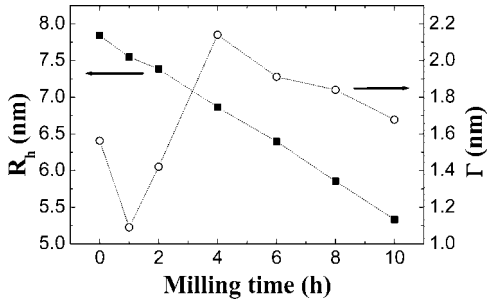

Figure 1. Evolution of PMMA hydrodynamic radius, R_h, and polydispersity, Γ, as a function of milling time (methyl ethyl ketone as solvent).

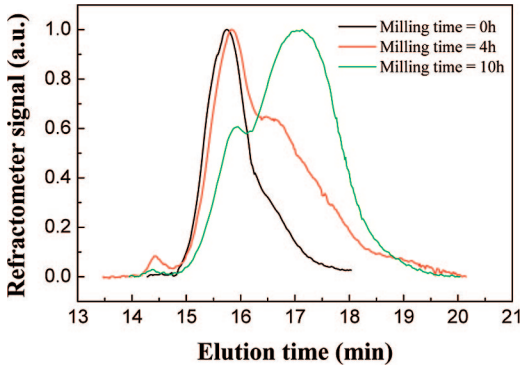

Figure 2. Normalized chromatograms obtained by SEC of PMMA milled for different times.

in molar mass after milling. Thus, if a random coil model in a thermodynamically good solvent is assumed for the PMMA (as methyl ethyl ketone is), it can be demonstrated that $M' = M_0(R'/R_0)^2$, where M is the average molecular weight of the polymer with hydrodynamic radius R' and the 0 subscript stands for the polymer without treatment. Therefore, taking the data obtained from DLS (Figure 1), it is possible to estimate that the average molecular weight decreases about 54% after 10 h of milling. These results clearly point out the chain scission that was considered in ref 25 but not confirmed experimentally there. In addition, SEC provides complementary information to DLS, as shown in Figure 2 where the normalized curves of the output signal from the refractometer as a function of milling time have been plotted. Here, the PMMA peak shifts to longer elution volumes and diminishes its height, whereas a new peak of smaller molecular weight arises, whose contribution becomes concomitantly higher. All these results prove undoubtedly the rupture of the polymeric chains caused by the HEBM and fully agree with those by Smith et al.,[31] who studied the effect of high-energy mechanical milling on PMMA at ambient and cryogenic temperatures.

Another interesting parameter to be analyzed is the polydispersity. This parameter has been included in Figure 1, where it can be observed how the distribution widens, undergoing an initial increase in Γ and followed by a decrease at highest milling times. The chromatograms (Figure 2) follow the same trend, also. These findings are in accordance with those reported by Smith et al.[31] However, in our case it is more clearly evidenced that the chromatogram peak broadens at intermediate milling times due to the appearance of a bimodal distribution, which finally tends to disappear at longer milling times.

To see the effect of ball milling (in terms of milling time) and the effect of temperature in the structure and conformation of the PMMA, IR absorption spectra of the polymer in the more sensitive region to conformational changes were collected. In particular, as an example, four normalized FTIR spectra

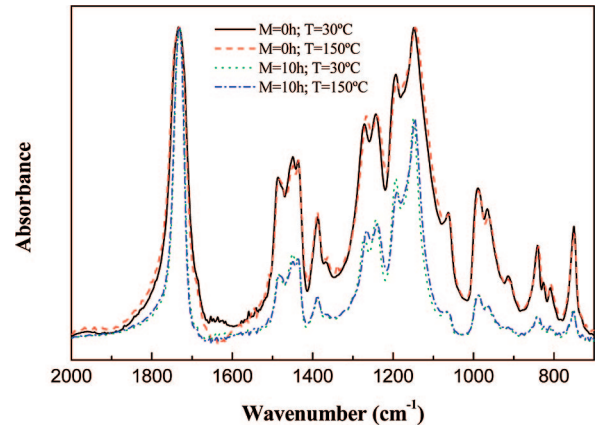

Figure 3. Absorption FTIR spectra of PMMA at 30 and 150 °C without further treatment and subjected for 10 h to high-energy ball milling.

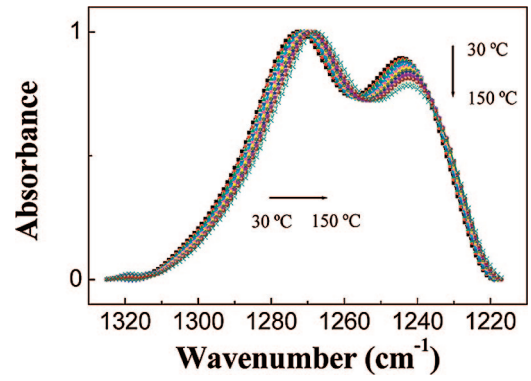

Figure 4. Evolution with temperature of the normalized IR absorption associated with the cis and trans ester group vibration, ν_a(C−C−O). Sample of PMMA milled for 2 h.

representing the extremes studied for those variables (temperature and milling time) are plotted in Figure 3.

Let us consider first the effect of temperature. This is reflected in small variations in the relative absorption peaks (see Figure 3). One example of this effect can be observed in the relative absorbance between the peaks centered at 1270 cm^{-1} (ν_1) and 1242 cm^{-1} (ν_2), which is clearly shown in Figure 4. These peaks were assigned by Nagai[26] and Willis et al.[32] to the ν_a(C−C−O) vibration, whereas Havriliak and Roman[27] pointed out that the splitting of this vibration into two components is a consequence of two rotational−isomeric states of the ester group, where the C−OCH_3 and C^{α}−CH_3 bonds are in mutual cis or trans orientation arising from the internal C^{α}−CO bond rotation (Figure 5).

From spectroscopic and ab initio studies of MMA, Owen et al.[33] and Konoka et al.[34] associate each band with one of the two conformers. The ab initio results have established that the high-frequency band (ν_1) is due solely to the trans conformation, whereas the low-frequency component (ν_2) is associated exclusively with the cis conformation. Thus, the corresponding polymer peaks ν_1 and ν_2, must be assigned to respectively the trans and cis conformation of the ester group (Figure 5). In view of that, if equilibrium between rotational isomers is considered, the ratio of the absorbances for the two peaks must be related to the conformational energy difference between the trans and cis rotational states by the van't Hoff equation.

Custom is to use curve fitting to analyze spectroscopic bands. Although generally it gives good results, sometimes these methods usually take the presence of theoretical bands whose existence is not completely ensured. Besides, it is necessary to assume a specific shape for the bands (Lorenzian, Gaussian,

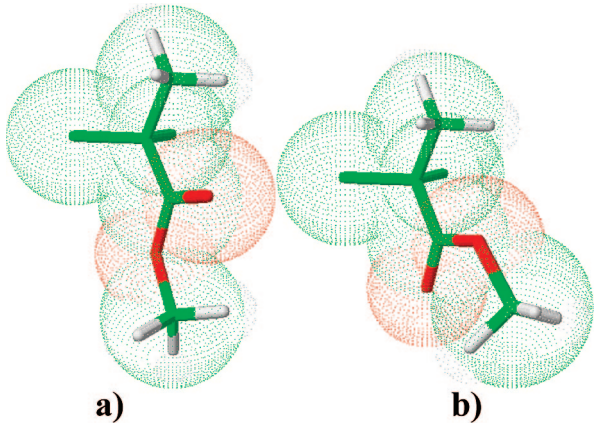

Figure 5. 3D models representing schematically the (a) trans and (b) cis rotational isomers causing the IR absorption peaks of the ester group at 1242 and 1270 cm^{-1}, respectively.

etc.). Because of this, it seems reasonable to try to extract information directly from the experimental data, with minimal baseline corrections and normalization for subsequently conducting proper comparisons. In this procedure the most important point is to follow a systematic way in the analysis of the bands, selecting the same intervals for baseline corrections, and keeping exactly the same method for obtaining a particular parameter to finally be able to compare changes in the spectroscopic bands. Indeed, these procedures might lead to distortions in the band shape, but if these are considered in the same way for all the spectra to be compared, the final conclusion should not be altered.

The plots in Figure 4 have been obtained after considering a baseline correction from 1217 to 1326 cm^{-1} and normalizing at the maximum of the peak centered at higher energy. It can be observed (i) a small peak shift to lower energies (about 5 cm^{-1} for the peak at 1270 cm^{-1} and about 2 cm^{-1} for the peak centered at 1240 cm^{-1}) and (ii) a relative absorbance increase of the peak centered at higher wavenumbers when the temperature increases.

Grohens et al.[35] associated the shift to higher frequencies in the ν_a(C−C−O) band at 1270 cm^{-1} to specific attractive interactions involving the methoxy group. In our case, when PMMA alone is considered, the shift of this band only can be due to changes in inter- or intramolecular interactions. Therefore, the results obtained suggest that heating the sample allows breaking, at least partially, those linkages (attractive interactions) by a simple thermal activation which might be moreover conditioned by changes in chain conformation. The fact that the ν_1 band shifts more than the ν_2 suggests that the trans conformation favors the attractive interactions involving the methoxy group with preference to the cis conformation.

Because of the small shift observed, about 5 cm^{-1} for the ν_1 band, and the resolution of the spectra, 4 cm^{-1}, the ν_1(C−C−O) bands were baseline corrected with a straight line built from 1258 to 1298 cm^{-1}. This helps to improve mathematically (indirectly) the resolution by using the first moment of the absorption band, $\langle\nu_1\rangle$. Specifically, the absorption bands were considered as distributions of energies prior to taking from them the first moment of the distribution.[36]

Figure 6 shows, as an example, a plot of $\langle\nu_1\rangle$ for the ν_1(C−C−O) band as a function of temperature. As can be expected from observation of Figure 4, the $\langle\nu_1\rangle$ decreases as temperature increases showing two slope changes, in particular at 55 °C (very smooth) and 115 °C, respectively, in the absence of milling (Figure 5). The first temperature matches that of the β-relaxation in PMMA[37,38] which suggests that the β-relaxation must be due to a motion activated at low energy, such as the

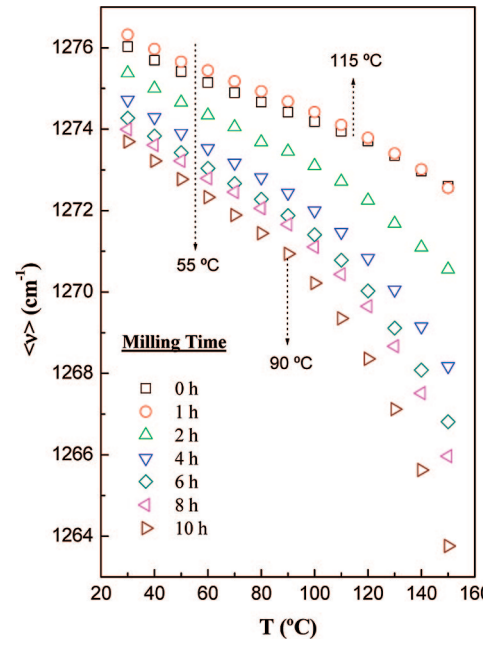

Figure 6. Evolution with temperature of the first moment of the band centered at 1270 cm^{-1} for the PMMA subjected to different milling times (0, 1, 2, 4, 6, 8, and 10 h).

Table 2. Values of Glass Transition Temperature, T_g, Obtained from the Plots of the First Moment of the Absorption Band as a Function of Temperature from the Vant' Hoff Plots, Together with the Conformational Energy Difference, ΔH, above and below T_g (PMMA Samples)

milling time (h)	T_g (°C) from ν_1 band shift	T_g (°C) from $A\nu_2/A\nu_1$ ratio	ΔH (cal mol^{-1}) $T < T_g$	ΔH(cal mol^{-1}) $T > T_g$
0	115	115	177 ± 7	786 ± 39
1	111	114	182 ± 5	730 ± 30
2	106	103	156 ± 8	732 ± 23
4	100	100	140 ± 10	782 ± 25
6	97	97	142 ± 10	771 ± 26
8	94	95	144 ± 9	771 ± 24
10	90	90	146 ± 13	840 ± 24

rotation around a bond of the pendant ester group, for instance. If the attractive interactions are considered to be due to contribution of the methoxy groups, the only way to change their positions to reduce the attractive interactions is by rotating the ester group around the axis which passes along the bond $C^{\alpha}-COOCH_3$. This assumption agrees with the results of Schmidt-Rohr et al.,[39] who suggested that the β-relaxation in PMMA consists of a 180° flip of the ester group about the C−CO bond. On the other hand, the second temperature observed as a change in the slope in Figure 6 coincides with the α-relaxation in PMMA or the glass transition temperature, T_g, obtained by DSC.[25] This relaxation is usually assigned to a cooperative motion of the backbone bonds, which is the other possible molecular movement that may reduce attractive interaction by putting apart the interacting groups each other.

In Figure 6 all milling times under study from 0 to 10 h have been included. In all the cases the same behavior as a function of temperature was observed although with some differences: (a) the temperature at which the second thermal transition occurs (T_g) decreases with milling time (Table 2) and (b) the slopes of the plots increase with milling time.

On the other hand, and considering what was stated above, result ii extracted from Figure 4 which accounts for the variation in the relative absorbance between the peaks ν_1 and ν_2 can be interpreted in terms of a population change between the two different rotational positions (temperature-induced cis−trans rotational isomerization of the ester group). In particular, the

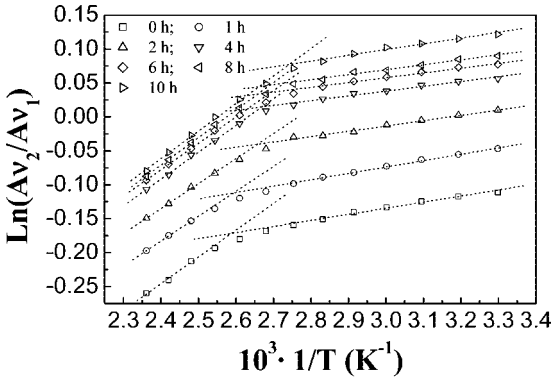

Figure 7. Van't Hoff plots in terms of absorbance ratios of the cis−trans rotational isomers of the ester group for the pure PMMA subjected at different milling times (0, 1, 2, 4, 6, 8, and 10 h).

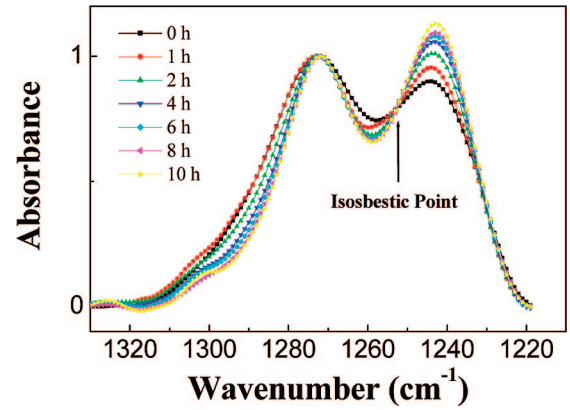

Figure 8. Evolution of the ν_a(C−C−O) band as a function of milling time for PMMA.

ratio of absorbances at 1240 and 1270 cm^{-1}, $A\nu_2/A\nu_1$, decreases as temperature increases. This result means taking into account the peaks assignation, that the increase in the temperature implies an enhancement of the trans content at expense of the cis content. The same behavior as a function of temperature is observed for all the milling times. Therefore, in order to study the effect of temperature and ball milling process in the PMMA macromolecular structure and conformation, these data were analyzed for the samples by using the van't Hoff equation as described in ref 40 at all milling times and plotted as shown in Figure 7. (In our case the absorbance ratios, $A\nu_2/A\nu_1$, were obtained from plots as those represented in Figure 4.)

It is clearly observed how the absorbance ratio $A\nu_2/A\nu_1$ changes its slope at a defined value of temperature that can be associated with the glass transition temperature, T_g, considering the values obtained for the same samples measured by differential scanning calorimetry (DSC).[25] The T_g for each sample (Table 2) were deduced from the intercept between the straight lines fitted in each part of the plots (Figure 7).

The conformational difference energies, ΔH, were then calculated from linear regression analysis (Table 2) having in all cases regression coefficients higher than 0.99. Two values of ΔH are then obtained for the same ester group, the lower one coming from data at temperatures below the T_g and the higher one obtained at temperatures above the T_g. In accordance with the experimental work by O'Reilly and Mosher[24] and with the theoretical work carried out by Vacatello and Flory[41] and Sundararajan,[42] these results point out that the conformational cis−trans energy difference strongly depends on the backbone conformation. Since backbone motions are assumed to be frozen at temperatures below T_g, the conformational energies calculated at those temperatures may only refer to changes in side-chain conformations. However, above the T_g, both the side-chain and the backbone motions are allowed, and therefore the calculated energies might reflect a cooperative movement.[23]

Furthermore, a possible extended explanation can be considered here. At relatively low temperature (at least 30 °C) only free ester groups (isolated, having no specific interactions), without other restrictions for its movement different than the proper rotation around a single bond, are allowed to isomerize. On the contrary, when the temperature is high enough, these ester groups intra- or intermolecularly interacting each other begin to rotate aided by the cooperative backbone motion occurring at temperature higher than T_g. This scheme would perfectly account for the interpretation made for the ester band shifts observed.

Let us consider now the effect of milling time. This variable has important consequences on the FTIR spectra. In Figure 6 it is observed that the higher the milling time is (i) for the same temperature the ν_1 band shifts toward slightly higher frequencies, (ii) the band shift is more important with temperature, and (iii) the change in the slope assigned to the T_g occurs at lower temperatures (Table 2).

Assuming the explanation put forward above, which accounts for restrictions in the ester group motion due to specific interactions, the first evidence suggests a conformational change induced by the ball milling, which would reduce the number of specific interactions or would make them to be weaker. The second evidence is concordant with the first one because the weaker the interactions between ester groups the more pronounced temperature effect on the band shift is expected. Finally, the reduction of T_g was elsewhere interpreted in terms of a reduction in the average molecular weight of the PMMA due to chain scission when the polymer is subjected to extremely high shear forces,[25,31] which completely agrees with what has been observed experimentally in this work by DLS and size exclusion chromatography.

Besides, Figure 3 shows that the relative absorbance of several bands also changes with milling time; in these cases other type of representations done with different normalization criteria aid to perceive better such changes. For instance, in the case of ν_1 and ν_2 bands similar plots as those shown in Figure 4 can be represented (Figure 8) in order to see whether the milling process exerts any population change between the two different rotational positions (rotational isomerization of the ester group). As can be seen in Figure 8, the ν_2 band increases at the expense of the ν_1 one with milling time, showing a clear equilibrium displacement to the cis conformation of the ester group. This result is in accordance, first, with the assumption of a ball milling-induced conformational change and, second, with the less number or weaker specific interactions if they are favored with the trans conformation, as suggested by the band shifting in Figures 4 and 6. Furthermore, it is worth highlighting in Figure 8 the presence of the isosbestic point, which is the most realistic evidence of the equilibrium that exists between the species absorbing at ν_1 and ν_2.

The T_g's at different milling times can be obtained from curve fitting of plots in Figure 7 (Table 2). As expected, a reduction on T_g with milling time is observed in good correspondence with the T_g values different from the ν_1 band shifts, leading to the same conclusion. On the other hand, the similar values for conformational difference energy, ΔH, above and below T_g regardless the milling time (Table 2) suggest that the ball milling process does not exert any change in the dynamic mechanism of the PMMA, at least within the experimental uncertainty in ΔH which might include small changes due to variation in weak specific interactions.

Another interesting observation from Figure 3 is that the width of the carbonyl band (1733 cm^{-1}) diminishes, and its relative

absorbance clearly increases with milling time. In addition, the width of the ν_1 band also decreases.

At this point, one could think that the PMMA particles within the KBr plates might lead to scattering phenomena producing partial absorption at the edge of the particles. Because of this, it is possible to think that as the particle size of the PMMA reduces as grinding proceeds, over-absorption and other effects might play a smaller role and the intensity relationships may become closer to those of thin film spectra. However, the spectra analysis presented here shows, among other things, the existence of an unambiguous isosbestic point and clear changes pointing to the glass transition temperatures (they perfectly match with those obtained by DSC). Therefore, we must conclude that these evidences do not seem to come from sample artifacts. On the other hand, these so alleged scattering effects should have been detected at higher wavenumbers, where the scattering is really important, and this has not been the case.

In thin film spectra, the C═O mode is the most intense in the spectrum.[24,43–48] However, from refs 24 and 43–48 important variations in the absorbance ratio between the carbonyl band and the highest peak of the group assigned to ester vibration can be plainly observed. In particular, this ratio has two clear dependences: one of them is the film thickness, and the other one is the tacticity of the PMMA. Therefore, these results point that the relative absorbances due to the vibration modes associated with the PMMA groups are highly dependent on their spatial disposition (conformations and configurations of the macromolecules). It is well-known that the polymer conformation can greatly change at its surface with respect to that in the bulk, and this may be the reason why important changes are observed as a function of film thickness.

The shape and widths of infrared bands are an important source of information about interactions and molecular dynamics.[49] In polymer spectroscopy, it is common to study the shapes and widths of the bands because they are related to the distribution of local environments experienced by radiation absorbing or emitting moieties, but the band due to a particular absorption or emission reflects the superimposition of different frequencies that are a result of interactions in slightly different local environments.[12,49,50] Therefore, the width reduction of the carbonyl and ester bands suggests that this group is the other counterpart responsible for the specific interactions appearing in the ester group and which are reduced as a consequence of the milling process. Again the experimental data are pointing out that the great shear forces applied to the polymer during the mill process exert a so dramatic change in the structure and conformation of the PMMA that the orientation between interacting groups gives up operating. In addition to this, the increase in the relative absorption of the carbonyl group probably reflects a higher change of dipole moment in its vibration if less specific interactions are affecting it.

3.2. Nanosilica-Filled PMMA. For comparison, the normalized spectra at the carbonyl peak for the pure PMMA and nanosilica-filled PMMA (silica-PMMA) are shown in Figure 9. These spectra were collected at 30 °C for the samples which underwent 10 h of ball milling.

In general, in the region shown in Figure 9, the FTIR spectra are practically the same except (i) for the interval from 980 to 1150 cm^{-1}, in which the contribution of the bands coming from the Si−O−Si stretching modes typical of silica are clearly observed, and (ii) for the carbonyl band which is slightly narrower in the silica-PMMA sample. These effects are better noticed in the difference spectrum (silica-PMMA−PMMA) shown as an inset in Figure 9.

Let us consider now the effect of temperature on the FTIR spectra for the samples of PMMA with silica nanoparticles. Once more, this effect can be observed: (i) in the relative

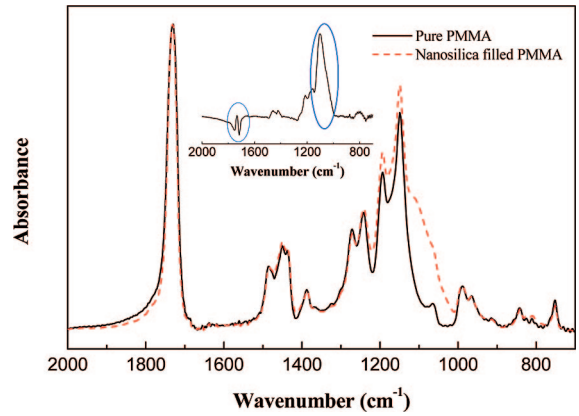

Figure 9. Normalized spectra at the carbonyl peak for the pure PMMA and nanosilica-filled PMMA (silica-PMMA) samples milled for 10 h. The spectra were collected at 30 °C.

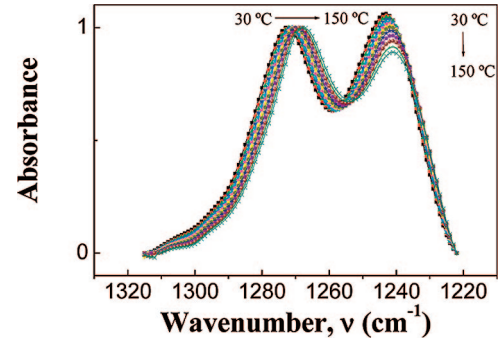

Figure 10. Evolution of the normalized IR absorption associated with the cis and trans ester group vibration, ν_a(C−C−O), with temperature for the sample silica-PMMA milled for 2 h.

absorbance between the peaks centered at 1270 cm^{-1} (ν_1) and 1242 cm^{-1} (ν_2) and (ii) in the ν_1 shifts clearly shown in Figure 10 in which, by normalizing the interval corresponding the ν_1 and ν_2 bands, similar plots to those of Figure 4 are represented showing the same behavior with temperature.

Figure 11 shows the plots for the values of $\langle\nu_1\rangle$ associated with the ν_1(C−C−O) band as a function of temperature when the PMMA is filled with nanosilica particles. As can be expected (Figure 10), $\langle\nu_1\rangle$ decreases as temperature increases, showing nearly two slope changes (Figure 11) as in the cases of milled PMMA without silica nanoparticles, and therefore, the same interpretation can be done for these PMMA-modified systems. However, when silica nanoparticles are within the polymer after the HEBM process, two important differences arise: (i) for a specific temperature and milling time, the values of $\langle\nu_1\rangle$ are slightly lower, and (ii) the second temperature onset for the $\langle\nu_1\rangle$ vs T plots, T_g's, reduces to some extent (Table 3).

If the position of the ν_1 band depends on the attractive interactions involving the methoxy and carbonyl groups, which are conditioned by changes in chain conformation as was stated before (they are favored by the trans conformation of the ester group), the slightly lower values of $\langle\nu_1\rangle$ in the silica-PMMA samples may be due to lower population of trans conformers. Since the presence of silica nanoparticles is the only difference between both kinds of samples, two possible explanations might account for this evidence: either specific interactions between silica nanoparticles and PMMA might induce cis conformation enhancement, or the presence of rigid silica nanoparticles might force slightly more chain scissions during the milling process, thus increasing the population of cis with respect to the trans conformers.

As previously shown (Figure 8), the milling process induces an increase in number of the cis conformers. Therefore, the

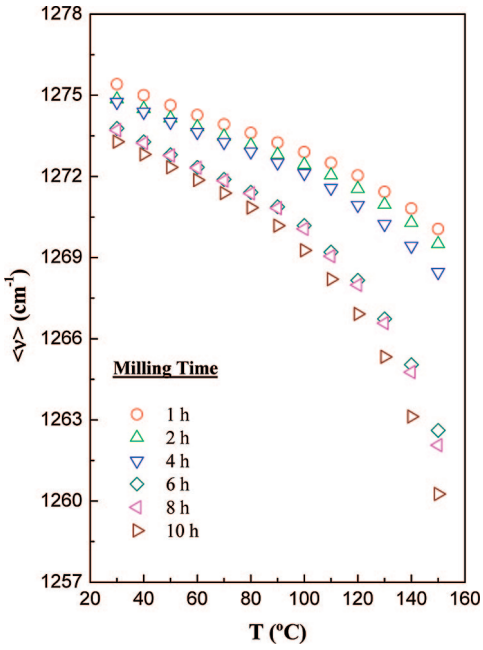

Figure 11. Evolution with temperature of the first moment of the band centered at 1270 cm^{-1} for the silica-PMMA sample subjected to different milling times (1, 2, 4, 6, 8, and 10 h).

Table 3. Glass Transition Temperature, T_g, Obtained from the Plots of the First Moment of the Band as a Function of Temperature and the Van't Hoff Plots, Together with the Conformational Energy Difference, ΔH, above and below T_g (Silica-PMMA Samples)

milling time (h)	T_g (°C) from ν_1 band shift	T_g (°C) from $A\nu_2/A\nu_1$ ratio	ΔH (cal mol^{-1}) $T > T_g$	ΔH (cal mol^{-1}) $T > T_g$
1	105	105	211 ± 14	1132 ± 30
2	107	106	187 ± 7	876 ± 21
4	100	96	205 ± 11	1087 ± 17
6	93	93	204 ± 9	1073 ± 27
8	88	87	221 ± 15	1084 ± 28
10	85	85	187 ± 15	1005 ± 21

second explanation seems to be more plausible since it would explain the slightly lower T_g's observed for the silica-PMMA samples. In fact, for a particular temperature and milling time the values of $A\nu_2/A\nu_1$ ratio are higher when the silica nanoparticles are present.

On the other hand, the van't Hoff plots in Figure 12 show how the $A\nu_2/A\nu_1$ ratio decreases with the temperature, which implies, as in the case of pure PMMA, the temperature produces an increase of the trans content with respect to the cis one. The same behavior as a function of temperature was observed for

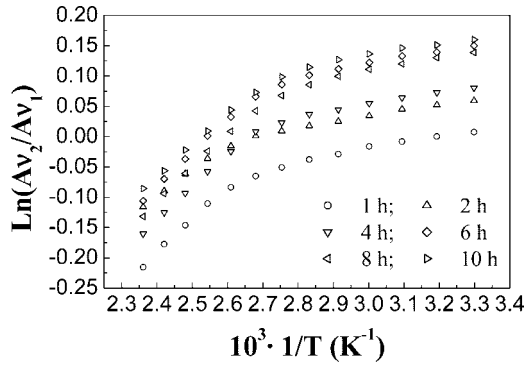

Figure 12. Van't Hoff plots in terms of absorbance ratios of the cis−trans rotational isomers of the ester group for the silica-PMMA sample subjected at different milling times (1, 2, 4, 6, 8, and 10 h).

all the milling times considered. Therefore, in the presence of dispersed silica nanoparticles, the effect of the HEBM in the macromolecular structure and conformation of PMMA can also be examined by fitting the experimental data via a van't Hoff equation[40] (Figure 12). In this case the absorbance ratios ($A\nu_2/A\nu_1$) were obtained from plots as those represented in Figure 10.

For the silica-PMMA samples and as in the case of PMMA without milling, it is clearly observed how the absorbance ratio $A\nu_2/A\nu_1$ changes its slope at a well-defined value of temperature that can be associated with the glass transition temperature.[25] The T_g values for each sample (Table 3) were obtained from the intercept between the straight lines fitted in each part of the plots. Once more, it is possible to see that in the presence of silica nanoparticles the values of T_g are slightly lower, indicating that the presence of rigid ceramic nanoparticles facilitates the polymer chain scission.

As in the case of pure PMMA, the conformational energies were calculated from linear regression analysis, having in all cases regression coefficients higher than 0.99 (Table 3). For the same ester group two values of ΔH were obtained, coming from data at temperatures below the T_g (the lower one) and above T_g (the higher one). As in the case of PMMA alone, the results point out a strong dependence of conformational cis−trans energy difference of the ester group on the backbone conformation, and a similar explanation is valid in this case. One important difference, however, can be detected in the data in Table 3; i.e., the conformational energies are about 33−35% higher when silica nanoparticles are within the PMMA. A possible explanation of this fact may be the stabilization of the trans conformation by means of specific interactions between the ester moieties through the carbonyl or the methoxy groups and the silanols of the silica nanoparticles. However, no experimental evidence was found to support this argument. In fact, the bands assigned to the carbonyl and ester groups seem to point out just the opposite since they narrow only to some extent and do not shift to the direction associated with the existence of attractive interactions (lower wavenumbers in the case of carbonyl band and higher ones in the case of ester band).

Another explanation for the increase in the conformational energy difference when the silica nanoparticles are within the PMMA is that the HEBM allows the spreading of the polymer onto the nanoparticles surface in such a way that an efficient coating is achieved due to a better macromolecular packing. This effective packing might be the cause of the polymer constraint nearby the nanoparticles surface, yielding therefore a reduction of the molecular mobility. Assuming this explanation one might conclude that the HEBM allows obtaining a very good mechanical adhesion between the silica nanoparticles and the PMMA. In fact, this good adhesion has been already experimentally confirmed by atomic force microscopy (AFM).[25]

With this explanation in mind one would expect higher values of T_g due to a restricted polymer motion. However, this evidence was not observed by FTIR. A possible reason may be that this technique is not sensible enough to evidence a second slope change between the T_g and 150 °C in the plots of Figure 12. However, the DSC experiments for the same samples[25] did show a double T_g, being one of them even higher than the typical T_g of PMMA at 115 °C. Although in ref 25 this higher T_g was speculated to be due to a fraction of PMMA with higher molecular weight, it seems now to be more reasonable to assign it to the fraction of PMMA packed more efficiently nearby the nanoparticles. In fact, this fraction with higher T_g was estimated[25] in 16% by weight in the whole polymer, which would imply a percentage of 0.14% of constrained polymer in the KBr disks for the FTIR experiments. Taking into account the absorbances measured from the PMMA spectra, such a small

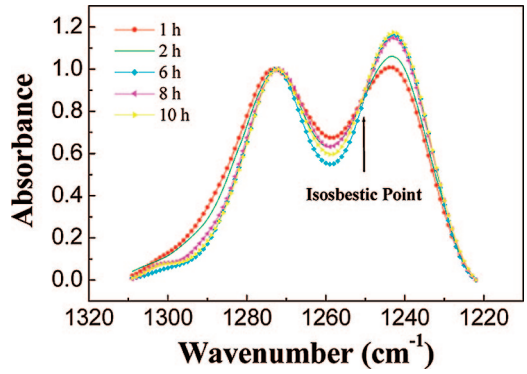

Figure 13. Evolution of the ν_a(C−C−O) band as a function of milling time for a silica-PMMA mixture.

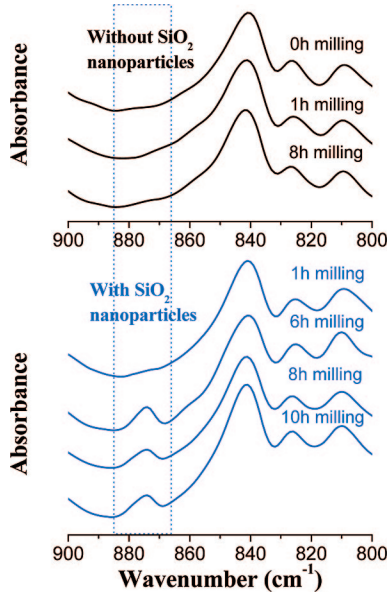

Figure 14. Effect of milling time on a selected region of the PMMA FTIR spectra where information about the backbone conformation can be extracted.

amount of constrained polymer would yield about 0.005 absorbance units for the ester groups, which is below the detection limit of the FTIR equipment.

The milling time effect has been also considered in the case of silica nanoparticle-filled PMMA (Figure 13). In this case the same general observation can be made, and therefore similar conclusions than in the case of pure PMMA can be extracted. However, when silica nanoparticles are present, the milling effect described in the case of PMMA alone seems to be more pronounced since $A\nu_2/A\nu_1$ ratios are higher for all the milling times. Once more, this result suggests that the presence of rigid ceramic particles slightly favors the polymer chain scission.

Finally, the region of the FTIR spectra where interesting information about backbone conformation can be found is shown in Figure 14. As mentioned in the Experimental Section, the absorption band at 860 cm^{-1} is characteristic for the all-trans or close to the all-trans conformation (TT), whereas the trans−gauche one (TG) absorbs at 843 cm^{-1} and is characteristic of the random coil.[28,30] In all the samples under study it was mainly observed the absorption at 842 cm^{-1}, pointing out that the most important backbone conformation is the TG. However, only in the samples with silica nanoparticles subjected to the milling process for more than 6 h a new peak at 874 cm^{-1} appears. If this peak is attributed to the existence of macromolecules with a highly trans conformation, one may think that the presence of such nanoparticles, in addition to the milling process, helps the polymer chain to adopt a specific conformation on the nanosilica surface, which consequently would allow the macromolecules to be more densely packed at the interface.

Conclusions

The effects of high-energy ball milling (HEBM) on the structure and interfacial conformations of PMMA in silica/PMMA nanocomposites have been studied. Results from DLS and SEC evidenced that PMMA subjected to HEBM at room temperature experiences chains scission, more extensively the longer the milling time is. The use of FTIR spectroscopy has shown (i) the existence of inter- and/or intramolecular specific interactions between ester groups that are conditioned by changes in chain conformation, the trans ester one favoring such interactions with preference to the cis conformation and disappearing by thermal activation, (ii) a T_g decrease of the PMMA when it is subjected to the HEBM process, and (iii) that the incorporation of silica nanoparticles within the PMMA by means of HEBM allows to achieve a good mechanical adhesion between them, generating an interface where the PMMA chains have a preferential backbone conformation which helps them to be better packed and therefore with restricted mobility.

Acknowledgment. The authors gratefully acknowledge the MEC of Spain for financial support (projects MAT2007-61607 and CTQ2006-14933/BQU).

References and Notes

(1) Yang, M.; Dan, Y. *Colloid Polym. Sci.* **2005**, *284*, 243–250.
(2) He, J.; Li, H.; Wang, X.; Gao, Y. *Eur. Polym. J.* **2006**, *42*, 1128–1134.
(3) Kinloch, A. J.; Mohammed, R. D.; Taylor, A. C.; Eger, C.; Sprenger, S.; Egan, D. *J. Mater. Sci.* **2005**, *40*, 5083–5086.
(4) Zhao, H. X.; Li, R. K. Y. *Polymer* **2006**, *47*, 3207–3217.
(5) Kim, S. H.; Kwak, S. Y.; Suzuki, T. *Polymer* **2006**, *47*, 3005–3016.
(6) Li, Y. Q.; Fu, S. Y.; Mai, Y. W. *Polymer* **2006**, *47*, 2127–2132.
(7) Yang, H.; Zhang, Q.; Guo, M.; Wang, C.; Du, R. N.; Fu, Q. *Polymer* **2006**, *47*, 2106–2115.
(8) Rong, M. Z.; Zhang, M. Q.; Zheng, Y. X.; Zeng, H. M.; Walter, R.; Friedrich, K. *Polymer* **2001**, *42*, 3301–3304.
(9) Rittigstein, P.; Priestley, R. D.; Broadbelt, L. J.; Torkelson, J. M. *Nat. Mater.* **2007**, *6*, 278–282.
(10) Ash, B. J.; Siegel, R. W.; Schadler, L. S. *Macromolecules* **2004**, *37*, 1358–1369.
(11) Bansal, A.; Yang, H.; Li, C.; Cho, K.; Benicewicz, B. C.; Kumar, S. K.; Shadler, L. S. *Nat. Mater.* **2005**, *4*, 693–698.
(12) Turrión, S. G.; Olmos, D.; Ekizoglou, N.; González-Benito, J. *Polymer* **2005**, *46*, 4023–4031.
(13) Keddie, J. L.; Jones, R. A. L.; Cory, R. A. *Europhys. Lett.* **1994**, *27*, 59–64.
(14) Van Zanten, J. H.; Wallace, W. E.; Wu, W. L. *Phys. Rev. E* **1996**, *53*, R2053–R2056.
(15) Forrest, J. A.; Dalnoki-Veress, K.; Stevens, J. R.; Dutcher, J. R. *Phys. Rev. Lett.* **1996**, *77*, 2002–2005.
(16) Fryer, D. S.; Peters, R. D.; Kim, E. J.; Tomaszewski, J. E.; Pablo, J. J.; White, C. C.; Wu, W. *Macromolecules* **2001**, *34*, 5627–5634.
(17) Roth, C. B.; McNerny, K. L.; Jager, W. F.; Torkelson, J. M. *Macromolecules* **2007**, *40*, 2568–2574.
(18) Ellison, C. J.; Torkelson, J. M. *Nat. Mater.* **2003**, *2*, 695–700.
(19) Keddie, J. L.; Jones, R. A. L.; Cory, R. A. *Faraday Discuss.* **1994**, *98*, 219–230.
(20) Fernandez, M. L.; Higgins, J. S.; Penforld, J.; Shackelton, C. S. *Polym. Commun.* **1990**, *31*, 124–127.
(21) Wu, W.; Majkrzak, C. F.; Satija, S. K.; Anker, J. F.; Orts, W. J.; Satkowski, M.; Smith, S. D. *Polymer* **1992**, *33*, 5081–5084.
(22) Konstadinis, K.; Thakkar, B.; Chakraborty, A.; Potts, L. W.; Tannenbaum, R.; Tirrell, M.; Evans, J. F. *Langmuir* **1992**, *8*, 1307–1317.
(23) Grohens, Y.; Brogly, M.; Labbe, C.; Schultz, J. *Polymer* **1997**, *38*, 5913–5920.
(24) O'Reilly, J. M.; Mosher, R. A. *Macromolecules* **1981**, *14*, 602–608.
(25) Castrillo, P. D.; Olmos, D.; Amador, D. R.; González-Benito, J. *J. Colloid Interface Sci.* **2007**, *308*, 318–324.
(26) Nagai, H. *J. Appl. Polym. Sci.* **1962**, *7*, 1697–1702.
(27) Havriliak, S.; Roman, N. *Polym. Prepr.* **1966**, *7*, 253–400.

(28) Chen, J.; Zheng, G.; Xu, L.; Zhang, J.; Lu, Y.; Xue, G.; Yang, Y. *Polymer* **2001**, *42*, 4459–4462.
(29) Grohens, Y.; Prud'homme, R. E.; Schultz, J. *Macromolecules* **1998**, *31*, 2545–2548.
(30) Spevacek, J.; Schneider, B.; Dybal, J.; Stokr, J.; Baldrian, J. *J. Polym. Sci., Part B: Polym. Phys.* **1984**, *22*, 617–635.
(31) Smith, A. P.; Shay, J. S.; Spontak, R. J.; Balik, C. M.; Ade, H.; Smith, S. D.; Koch, C. C. *Polymer* **2000**, *41*, 6271–6283.
(32) Willis, H. A.; Zichy, V. J. I.; Hendra, P. J. *Polymer* **1969**, *10*, 737–746.
(33) Baker, B. L.; Orgill, M. K.; Owen, N. L.; Stephenson, E. H.; Williams, G. A.; MacDonald, J. N.; Boggs, J. E. *J. Mol. Struct.* **1995**, *356*, 95–104.
(34) Tsuji, T.; Ito, H.; Takeuchi, H.; Konaka, S. *J. Mol. Struct.* **1999**, *475*, 55–63.
(35) Grohens, Y.; Schultz, J.; Prud'homme, R. E. *Int. J. Adhes. Adhes.* **1997**, *17*, 163–167.
(36) Mikes, F.; González-Benito, J.; Serrano, B.; Bravo, J.; Baselga, J. *Polymer* **2002**, *43*, 4331–4339.
(37) Hammerschmidt, J. A.; Gladfelter, W. L. *Macromolecules* **1999**, *32*, 3360–3367.
(38) Bistac, S.; Schultz, J. *Int. J. Adhes. Adhes.* **1997**, *17*, 197–201.
(39) Schmidt-Rohr, K.; Kulik, A. S.; Beckham, H. W.; Ohlemacher, A.; Pawelzik, U.; Boeffel, C.; Spiess, H. W. *Macromolecules* **1994**, *27*, 4733–4745.
(40) Tretinikov, O. N.; Ohta, K. *Macromolecules* **2002**, *35*, 7343–7353.
(41) Vacatello, M.; Flory, P. J. *Macromolecules* **1986**, *19*, 405–415.
(42) Sundararajan, P. R. *Macromolecules* **1986**, *19*, 415–421.
(43) Lade, R. J.; Morley, I. W.; May, P. W.; Rosser, K. N.; Ashfold, M. N. R. *Diamond Relat. Mater.* **1999**, *8*, 1654–1658.
(44) Shin, H. S.; Lee, H.; Jun, C.; Jung, Y. M.; Kim, S. B. *Vib. Spectrosc.* **2005**, *37*, 69–76.
(45) Shin, H. S.; Jung, Y. M.; Oh, T. Y.; Chang, T.; Kim, S. B.; Lee, D. H.; Noda, I. *Langmuir* **2002**, *18*, 5953–5958.
(46) Tretinnikov, O. N.; Ohta, K. *Macromolecules* **2002**, *35*, 7343–7353.
(47) Tretinnikov, O. N.; Zhbankov, R. G. *J. Mater. Sci. Lett.* **1991**, *10*, 1032–1036.
(48) González-Benito, J.; Koenig, J. L. *Macromolecules* **2002**, *35*, 7361–7367.
(49) Painter, P.; Sobkowiak, M.; Park, Y. *Macromolecules* **2007**, *40*, 1730–1737.
(50) Moron, R. L.; Olmos, D.; González-Benito, J. *Compos. Sci. Technol.* **2006**, *66*, 2758–2768.

MA800260K